MODELING REFRACTION ARRIVALS

Jeff Thorson

Abstract

With the right placement of a source in a suitable velocity model it should be possible to model head waves using a wave equation propagator - for instance, the telescope equation. In fact, examples in this paper do show such a refraction arrival. Another way to model refractions is the method given in the paper "Upward Continuing Head Waves" included in this volume. The idea is to create a moving point source along the velocity interface that simulates the head wave propagating in the faster velocity medium. This way, the strength of the refraction arrival can be tuned relative to the strength of the reflection arrival.

The refraction filter

Consider a horizontal interface between two rocks of different velocities. Intuitively, the head wave propagating upward from this interface is generated by a horizontally moving wave, which in turn is generated by an "exploding reflector." The point diffractor by itself gives a normal hyperbolic event in the (x,t) domain at the surface, and the horizontal wave at the interface will add straight line segments tangent to two symmetric points on the hyperbola.

A valid refraction-generating model then would be to assign to each "normal" point source at time $t = 0$ two expanding point sources starting at time $t = 0$ and moving outward from the scatterer at a velocity equal to that of the lower medium. This is recognized as a simple (though

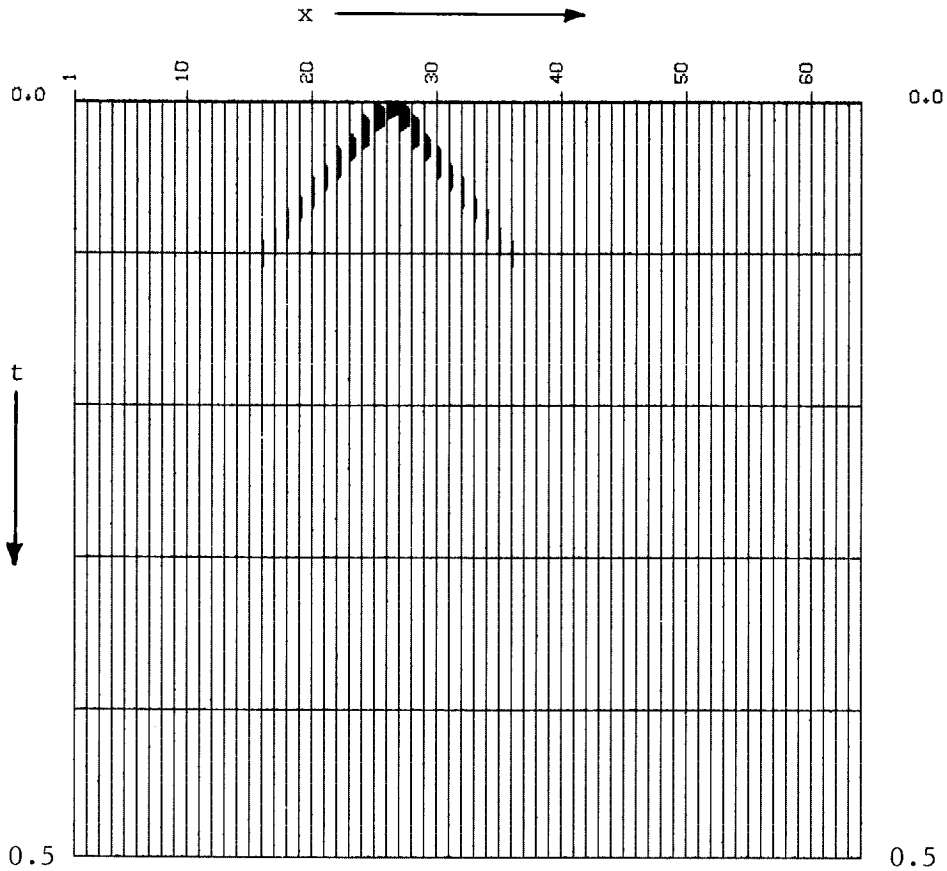

FIGURE 1.--Impulse response of refraction filter (1). Impulse at trace 26, time 0. $\varepsilon = 0.005$. v = 5000 ft/sec. dx between traces = 50 ft.

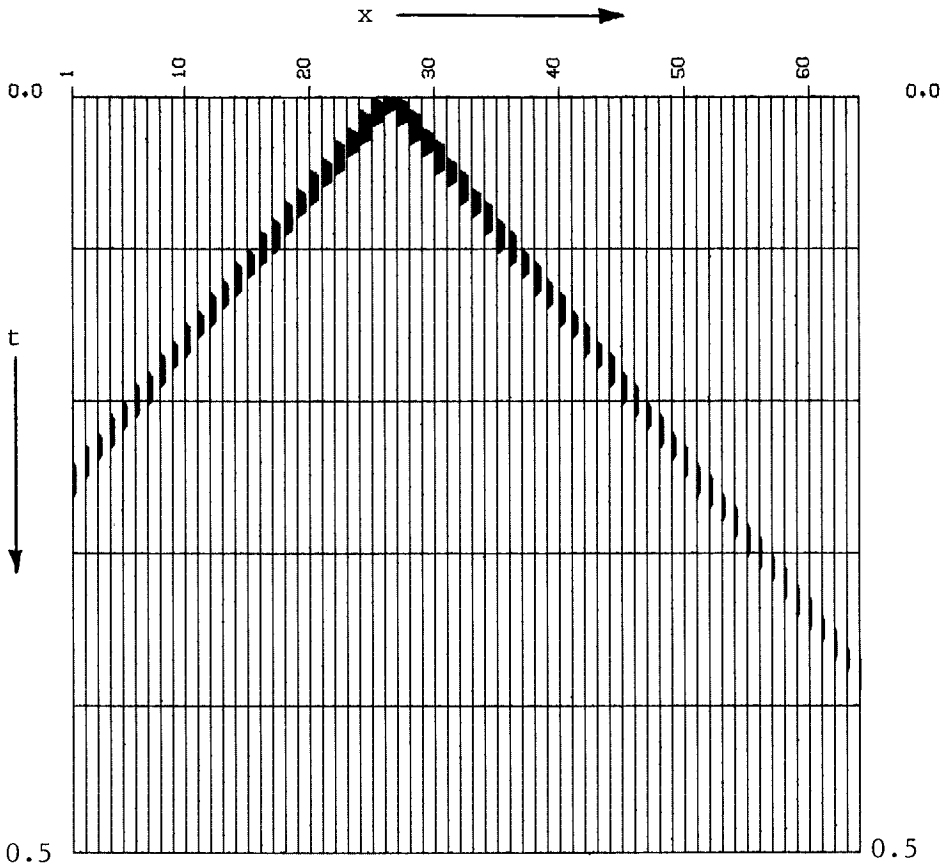

FIGURE 2.--Impulse response of refraction filter (1). Impulse at trace 26. $\varepsilon = 0.001$, v = 5000 ft/sec. dx = 50 ft.

possibly time-consuming) filter in the (x,t) domain, to be applied to our explosive reflector model before upward continuation is done with some operator.

Here is a modified version of the refraction filter given by Jacobs (see Jacobs and Claerbout, "Downward-and Upward-Continuing Head Waves," this report).

$$f(x,t) = \rho e^{-\varepsilon|x|}\, \delta\left(t - \frac{|x|}{v}\right) \tag{1}$$

The velocity of the faster medium is v, and ρ is an arbitrary scaling factor in weighting the refractions relative to the original scatterer. Note that $\delta[t - (|x|/v)]$ represents two impulses traveling away from each other, starting together at $t = 0$. An exponential damping factor of $e^{-\varepsilon|x|}$ is applied to the refraction source so that head waves die off after some suitable distance in x.

Two examples of the impulse response of this filter are given: Figure 1 represents an epsilon of 0.005 while Figure 2 represents a smaller epsilon of 0.0001, or one-fifth of the decay rate of Figure 1. The displays were calculated in the (x,t) domain: wraparound in x is not present.

If Equation (1) is transformed into the (k_x,ω) domain, the filter becomes the multiplicative factor

$$f(k_x,\omega) = \frac{2\rho\left(\varepsilon + i\,\frac{\omega}{v}\right)}{\left(\varepsilon + i\,\frac{\omega}{v}\right)^2 + k_x^2} \tag{2}$$

Examples

Figures 3 and 4 were made using the following model ("*" represents a source):

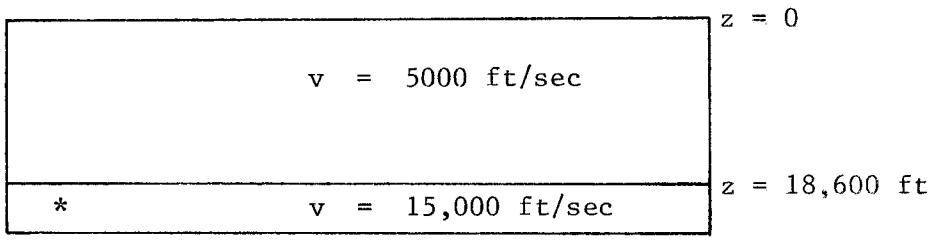

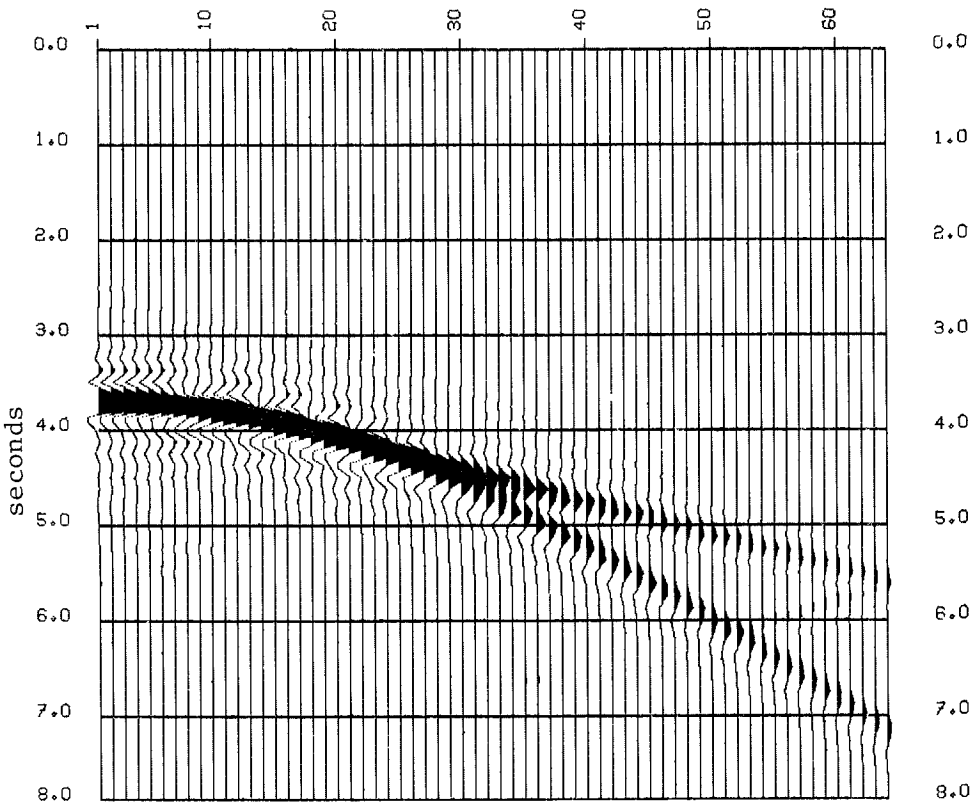

FIGURE 3.--Diffraction hyperbola with refraction arrival. nx = nz = nt = 64. dx = 500 ft. dz = 300 ft. dt = .125 sec. ρ = .0002. ε = .0001. Figures 3, 4, 5 and 7 all use the same parameters, except as noted in their captions.

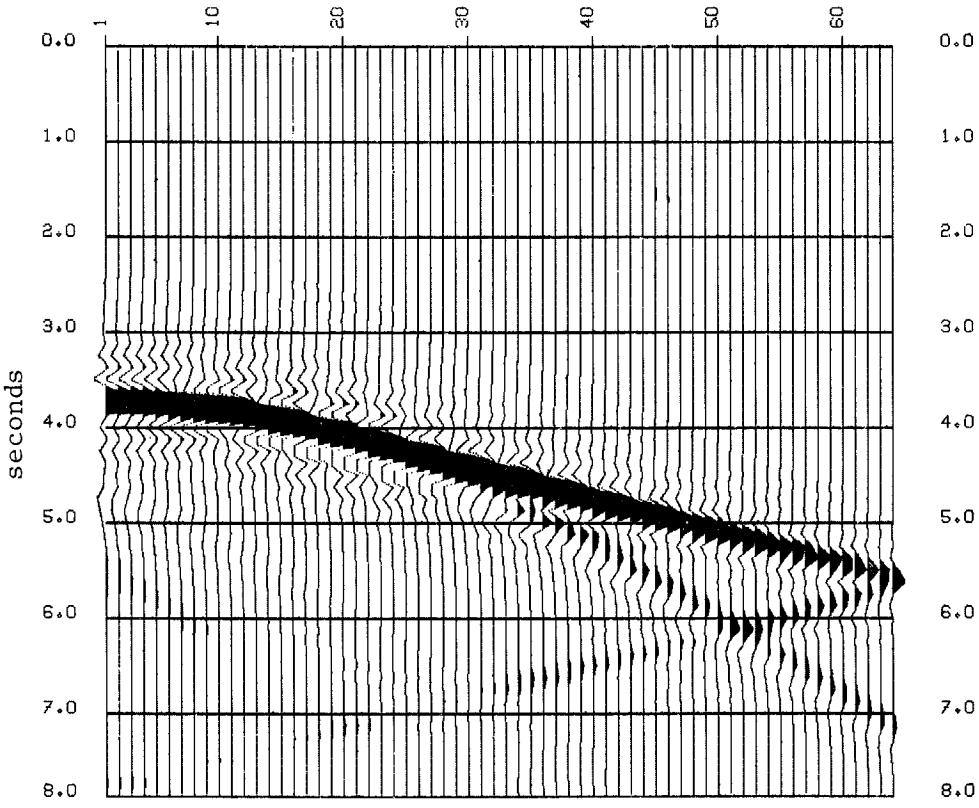

FIGURE 4.--Same as Figure 3, except refraction arrival is now four times as strong. Wraparound of the refraction is evident. ρ = .0008.

The point source was filtered with Equation (2), then propagated upward using the telescope equation. Since (2) is frequency dependent, the filtering step has to be done concurrently with the propagation step.

The parameters for Figure 3 are:

$$\left\{\begin{array}{l} nx = nz = nt = 64; \quad \rho = .0002; \quad \epsilon = .0001 \\ dx = 500; \quad dz = 300; \quad dt = .05; \end{array}\right\}$$

Figure 4 is identical to 3 except $\rho = .0008$, and the refraction has a corresponding increase in amplitude relative to the hyperbola of the point source. It can be seen that the refraction contributes a large amount of energy to the hyperbola even before it separates from the reflector. Observe Figure 5, however, which was generated from a model with the fast velocity now 10,000 ft/sec rather than 15,000 ft/sec. There is hardly any change at all in the waveform at the critical point -- which is counter to what one would expect from theory. Possibly the refraction filter could be further modified to accurately model the phase shift expected at the critical angle.

Figure 6 is a three-layer model.

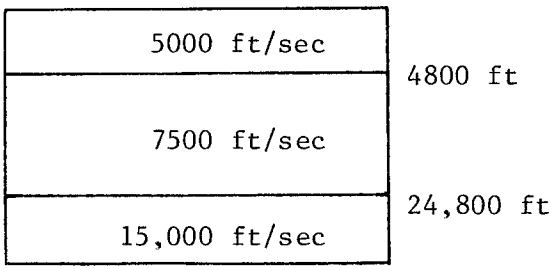

Note the refraction from the shallow layer seems to have died off before the deep refraction has even reached the critical angle.

Refractions generated without use of filter (2)

It is to be expected that if a one-way propagation scheme is used that can handle waves traveling in a direction right up to 90 degrees (horizontally), one should be able to see refraction arrivals, though possibly weak. This is because the source for a head wave in our case consists of energy traveling horizontally (for flat beds). If the propagation operator can handle horizontal energy without too much attenuation, this energy will give rise to head waves that should be seen. As

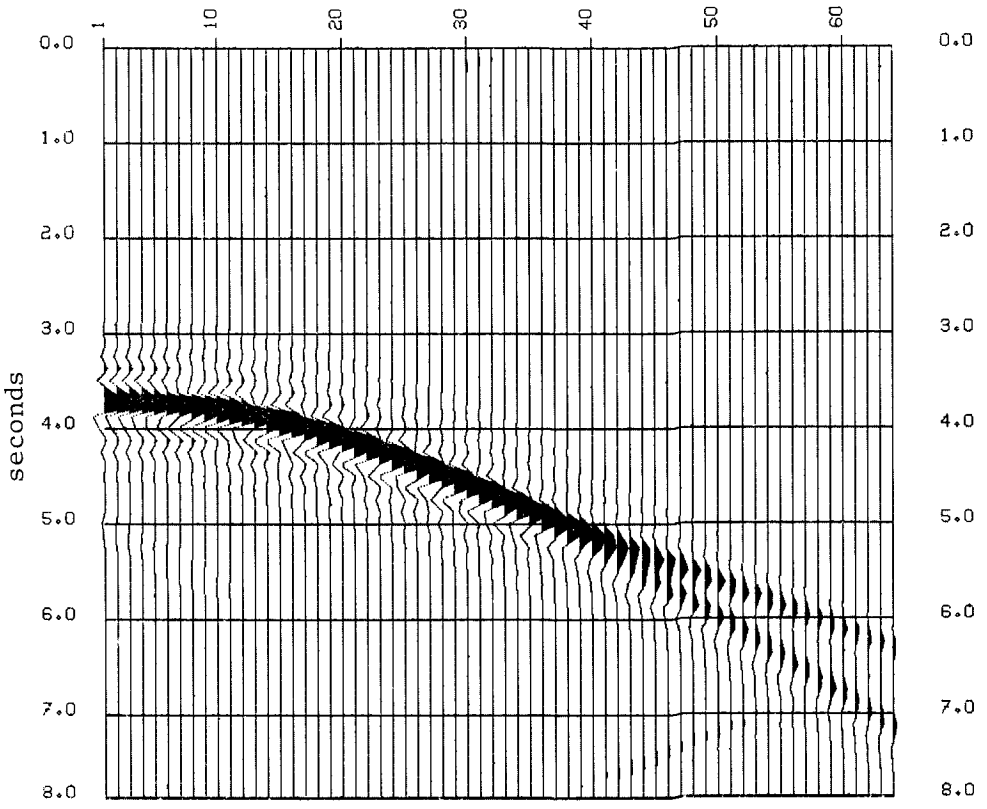

FIGURE 5.--Same as Figure 3, but velocity of the lower layer is now 10,000 ft/sec. The refraction leg branches off at a higher offset now.

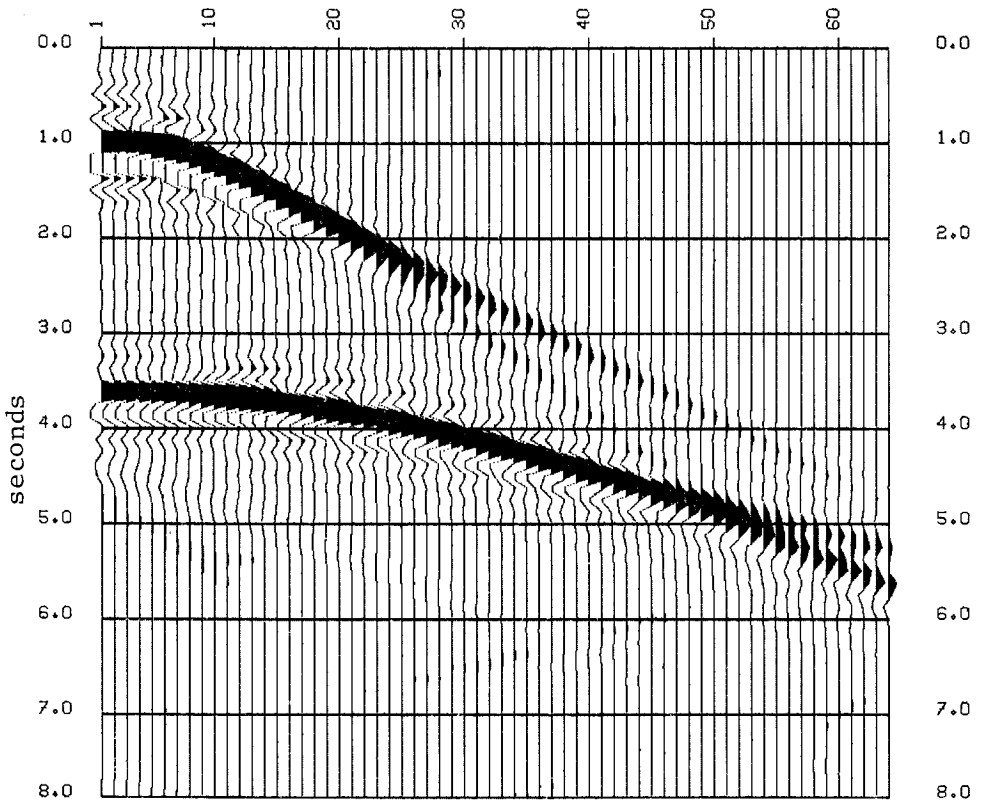

FIGURE 6.--Three-layer model:
v_1 = 5000 ft/sec
v_2 = 7500 ft/sec
v_3 = 15,000 ft/sec
dx = 500 ft
dz = 400 ft
dt = 0.125 sec

a matter of fact, if the telescope equation is used as the operator, they are seen. The model used to generate Figure 7 is

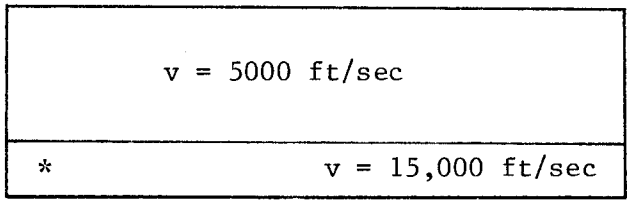

It is stressed that filter (2) was *not* applied in the case of Figure 7, but the weak refraction leg is solely due to energy that propagated from the sources along the interface at a velocity of 15,000 ft/sec.

The telescope equation was used to propagate, since it obeys the dispersion relation of the wave equation exactly up to 90 degrees. It is doubtful whether one would see the refraction leg of Figure 7 using a 45-degree or other tridiagonal-type operator, since they can hardly be expected to treat horizontal energy at all.

Figure 8 shows an (x,z) plot of a single frequency used in making up Figure 7. Though weak, the planar head waves can be seen. The interference effects they cause with the expanding cylindrical wave are readily visible.

Modeling Real Data

The next example is an attempt to accurately model real data. Figure 9 is a common midpoint gather from the Flemish Cap region off Newfoundland. The seafloor refraction can be seen quite clearly, along with other deeper events. Are these head waves radiating from sediment-sediment interfaces, or are they simply high-velocity reflections?

A slope and intercept were taken from the event at approximately trace 38, 1.2 seconds, and assuming that it is a refraction, velocities and depths for a two-layer earth model were computed. The model is shown at the bottom of Figure 10, which is the resulting synthetic gather generated by the model. There is good timing correspondence between the seafloor reflection and refraction of Figures 9 and 10, although amplitudes are not quite right.

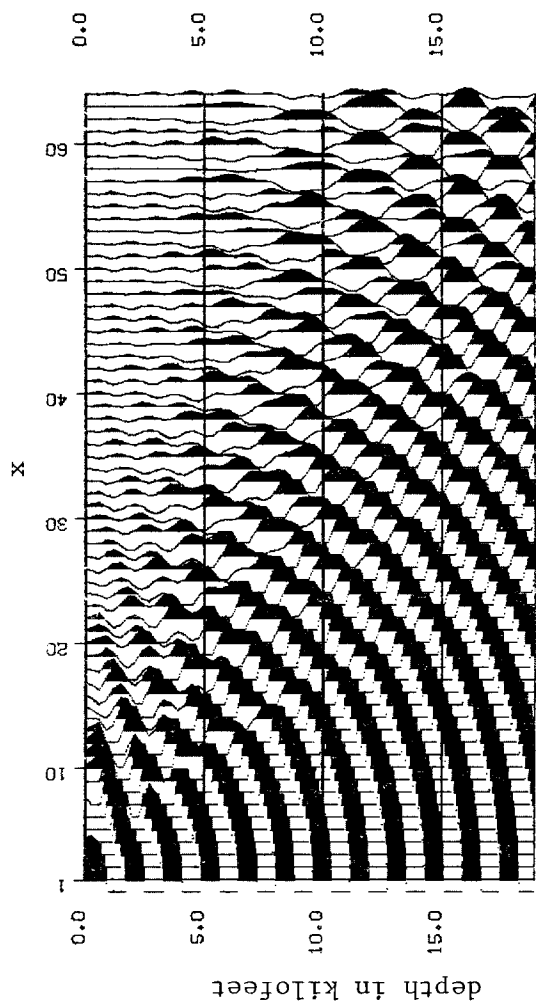

FIGURE 8.--A frequency component used for Figure 7. ω = 20 Hz. This actually models the downgoing wave for a source at depth zero.

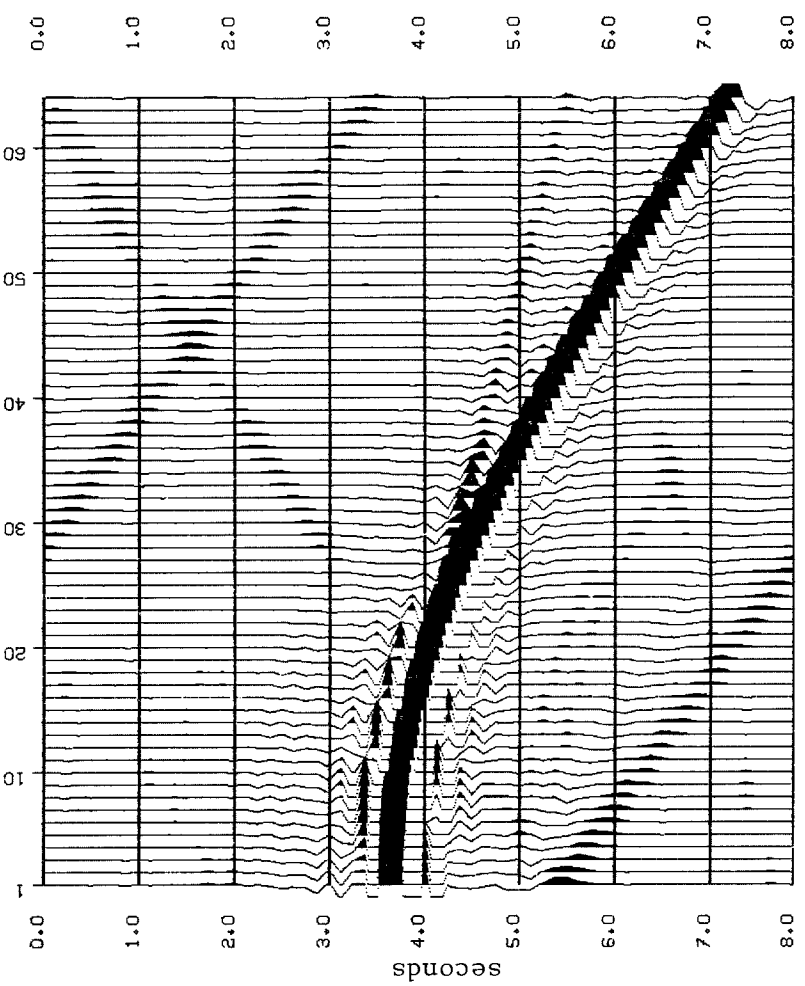

FIGURE 7.--Refraction event generated by the telescope equation without use of filter (2). The plot had to be gained up to see the weak event; the spurious events are wraparound effects.

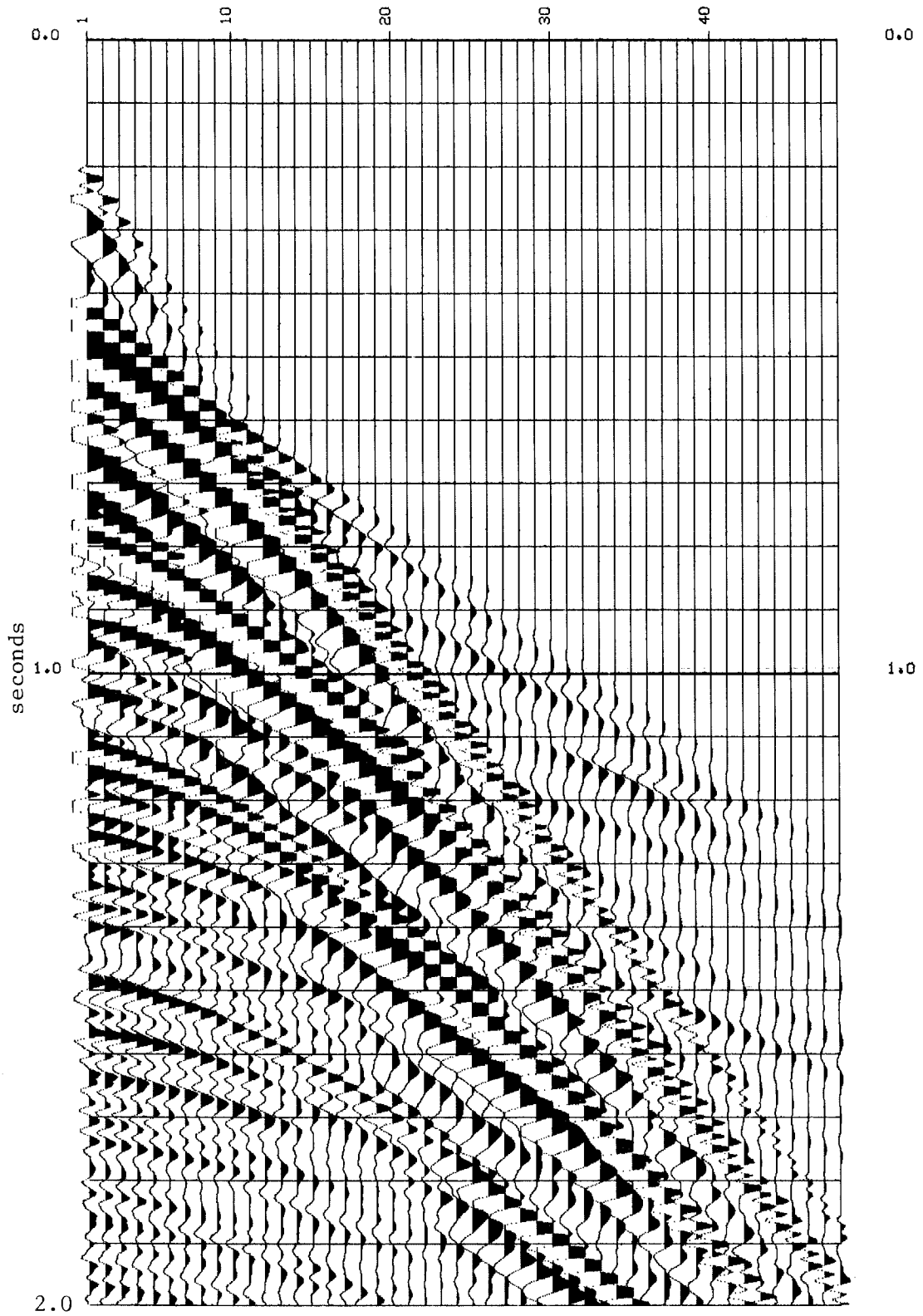

FIGURE 9.--Common-midpoint gather, marine data, offshore Newfoundland.

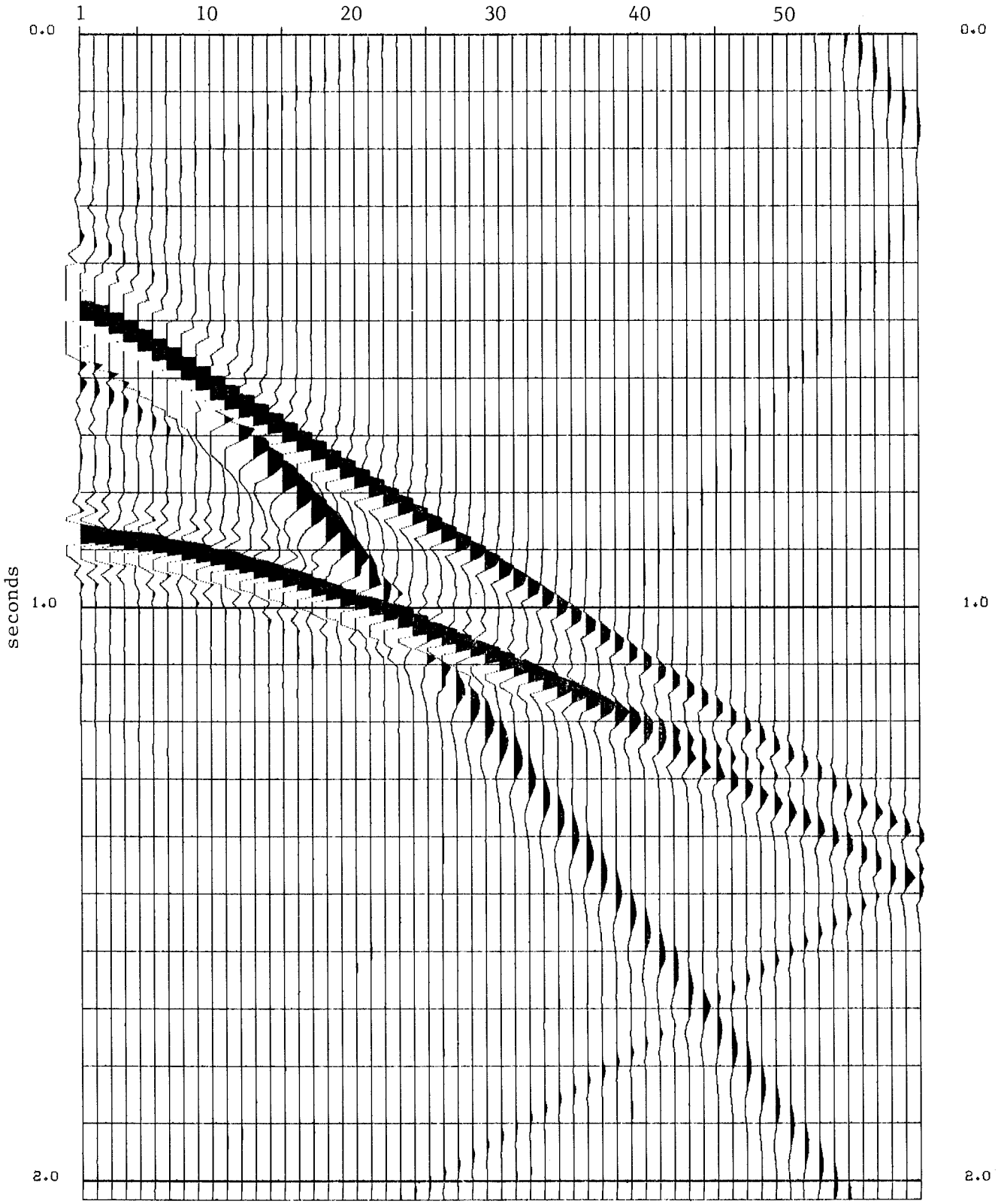

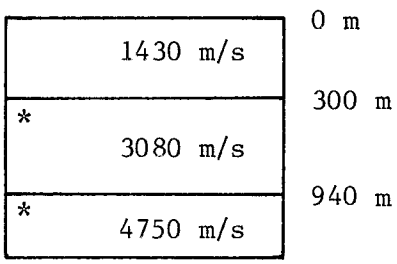

FIGURE 10.--Modeling the data of Figure 9. The water bottom refraction is strong and splits off at a near offset. The deeper refraction branches off at a much greater offset, and is weaker. ρ = .005. ε = .007.

The model shows the deep refraction splitting off from its reflection at about offset trace 40. Both the reflection and the refraction arrivals are in the region thought to be dominated by refractions on the original dataset. This example shows that the events out on trace 38 of the field gather (Figure 9) could just as well be reflections as refractions for the velocity model that was considered.

Summary

By applying refraction modeling to a real dataset, the seafloor refraction arrival can be accurately picked. The deeper the interfaces, however, the less effect the refraction arrival has on the data, because (1) refractions branch off of reflectors at farther offsets, and (2) they are nearly parallel to the reflections anyway. In any case, these effects can be modeled by the procedure outlined in this paper.